

Graviton production with 2 jets at the LHC in large extra dimensions

Kaoru Hagiwara^a, Partha Konar^{b,c,1}, Qiang Li^{c,2}, Kentarou Mawatari^{d,3}, and Dieter Zeppenfeld^{c,4}

^a *KEK Theory Division and Sokendai, Tsukuba 305-0801, Japan*

^b *Institute for Fundamental Theory, University of Florida, Gainesville, FL 32611, USA*

^c *Institut für Theoretische Physik, Universität Karlsruhe, Postfach 6980, D-76128 Karlsruhe, Germany*

^d *School of Physics, Korea institute for Advanced Study, Seoul 130-722, Korea*

¹ *E-mail: konar@phys.ufl.edu*

² *E-mail: qliphy@particle.uni-karlsruhe.de*

³ *E-mail: kentarou@kias.re.kr*

⁴ *E-mail: dieter@particle.uni-karlsruhe.de*

ABSTRACT: We study Kaluza-Klein (KK) graviton production in the large extra dimensions model via 2 jets plus missing transverse momentum signatures at the LHC. We make predictions for both the signal and the dominant Zjj and Wjj backgrounds, where we introduce missing P_T -dependent jet selection cuts that ensure the smallness of the 2-jet rate over the 1-jet rate. With the same jet selection cuts, the distributions of the two jets and their correlation with the missing transverse momentum provide additional evidence for the production of an invisible massive object.

KEYWORDS: Beyond Standard Model, Large Extra Dimensions, Hadronic Colliders..

Contents

1. Introduction	1
2. Calculations	2
3. Results and Discussions	4
4. Summary	8

1. Introduction

A general expectation in high energy physics today is that physics beyond the standard model (BSM) should emerge at TeV energies. This belief is founded on the observation that the electroweak symmetry breaking scale of the SM cannot be made stable against quantum corrections without invoking new physics at the TeV scale. With this in mind, an enormous international effort is being poured into the construction of the 14-TeV Large Hadron Collider (LHC) at CERN. Apart from supersymmetry (SUSY), models with large extra space dimensions, such as the one proposed by Arkani-Hamed, Dimopoulos, and Dvali (ADD) [1], provide an alternative possibility in this direction that is most exciting.

In the $D = 4 + \delta$ dimensional ADD model, the SM particles live in the usual 3+1-dimensional space, while gravity can propagate into the additional δ -dimensional space, which is assumed for simplicity to be compactified on the δ -dimensional torus T^δ with a common radius R . Then the 4-dimensional Planck scale M_{Pl} is related to the fundamental scale M_s as follows [1]:

$$M_{Pl}^2 = 8\pi R^\delta M_s^{\delta+2}, \quad (1.1)$$

where $M_s \sim \text{TeV}$ is possible for large compactification radius R . According to Eq. (1.1), one can expect that deviations from the usual Newtonian gravitational force law will appear at a distance around $R \sim 0.83 \times 10^{-16 + \frac{30}{\delta}} \text{mm} (2.4 \text{TeV}/M_s)^{1 + \frac{2}{\delta}}$. Terrestrial experiments gave the limit $R \leq 0.2 \text{ mm}$ by probing gravitational forces directly [2]. For $\delta = 2$ this translates into $M_s \gtrsim 1.5 \text{ TeV}$, while for $\delta > 2$, there are no strong limits on M_s .

In our four dimensional space-time, there appear Kaluza-Klein (KK) towers of massive spin-2 gravitons in the ADD model which interact with the SM fields. The interaction Lagrangian is given by [3, 4]

$$\mathcal{L}_{int} = -\frac{1}{\overline{M}_{Pl}} \sum_{\vec{n}} G_{\mu\nu}^{(\vec{n})} T^{\mu\nu}, \quad (1.2)$$

where the massive gravitons are labeled by a δ -dimensional vector of positive integers, $\vec{n} = (n_1, n_2, \dots, n_\delta)$, $\overline{M}_{Pl} = M_{Pl}/\sqrt{8\pi} \sim 2.4 \times 10^{18} \text{ GeV}$ is the reduced four dimensional Planck scale,

and $T_{\mu\nu}$ is the energy-momentum tensor of the scattering fields. The \vec{n} -th KK mode graviton mass squared is $m_{(\vec{n})}^2 = |\vec{n}|^2/R^2$. From Eq. (1.2) one can derive the relevant Feynman rules, some of which can be found in Ref. [3, 4]. For $M_s = 1$ TeV and $\delta = 4, 6$ and 8 , the mass gap of the KK modes is $\Delta m = R^{-1} \simeq 20$ keV, 7 MeV and 0.1 GeV [3], respectively. Thus the spectrum of KK modes can be treated as continuous for $\delta \leq 6$, and approximated by the mass density function [3]

$$\rho(m) = S_{\delta-1} \frac{\overline{M}_{Pl}^2}{M_s^{2+\delta}} m^{\delta-1}, \quad \text{with } S_{\delta-1} = \frac{2\pi^{\delta/2}}{\Gamma(\delta/2)}. \quad (1.3)$$

So far the strongest constraints for $\delta < 4$ extra dimensions come from astrophysics and cosmology, but they can be relaxed and do not diminish the importance of collider phenomenology [5]. We therefore discuss the $\delta = 3$ case as well. In collider experiments, there are two classes of effects that can probe large extra dimensions: virtual KK tower exchange between the SM particles and a real graviton emission. Since the couplings of the graviton with matter are suppressed by inverse power of \overline{M}_{Pl} , graviton direct production leads to missing energy signals. Detailed studies have been performed at LEP [6] and the Tevatron [7], by searching for gravitons in the processes $e^+e^- \rightarrow \gamma(Z) + E^{\text{miss}}$ and $p\bar{p} \rightarrow \gamma(\text{jet}) + P_T^{\text{miss}}$. The combined LEP 95% CL limits are $M_s > 1.60, 1.20, 0.94, 0.77, 0.66$ TeV for $\delta = 2, \dots, 6$ respectively, and the Tevatron 95% CL limits are $M_s > 1.18, 0.99, 0.91, 0.86, 0.83$ TeV. For the LHC, graviton production with a monojet has been investigated in detail and found to have strong ability to probe up to much higher extra dimension scale [8]. There is very little information on the underlying physics, however, in the transverse momentum and the rapidity of the single jet. One may thus wonder whether additional jets in graviton production can be used as a more sophisticated probe.

In this paper, we study graviton production with 2 jets at the LHC in large extra dimensions, in comparison with the dominant Zjj background [9], and examine if the 2-jet rate and correlations can give us more information about the mass scale of the missing object, in addition to the missing P_T distribution. At the same time we address the questions to what extent high transverse momentum graviton production will indeed emerge as a monojet signature. We will show that higher order QCD effects do lead to a more complex event structure, with multiple jets in the 100 GeV P_T range. The remainder of this work is organized as follows: In Section II we present the calculations. In Section III we give numerical results and discussions. Section IV contains our conclusions.

2. Calculations

We are considering the QCD production of a graviton with 2 jets at the LHC, $pp \rightarrow jjG_n$, including all the possible subprocesses, among which $gg \rightarrow ggG_n$, $gq \rightarrow gqG_n$ and $qq^{(\prime)} \rightarrow qq^{(\prime)}G_n$ play the most important role. Representative Feynman diagrams are shown in Fig. 1. In addition to the QCD processes of Fig. 1, we have also calculated the electroweak (EW) contributions to jjG_n production. In particular, we have determined the graviton production cross sections from weak boson fusion (WBF) processes. However, the WBF cross sections for jjG_n production represents a small correction, which is below 1%, even when imposing typical cuts to enhance

WBF over QCD sources [10]. Thus, WBF processes do not appear as a promising avenue for studying graviton production at the LHC, and we do not include them in the results below.

Significant background can come from any processes leading to two jets and missing transverse momentum, among which we consider the most important one, namely Zjj production with subsequent decay $Z \rightarrow \nu\bar{\nu}$ [9]. We also studied another class of processes which could be significant at least when missing P_T is not too large. This can arise from QCD production of Wjj with subsequent decay $W^\pm \rightarrow l^\pm\nu$ when the charged leptons $l = e, \mu, \tau$ are not identified. Here we follow the procedure of Ref. [10].

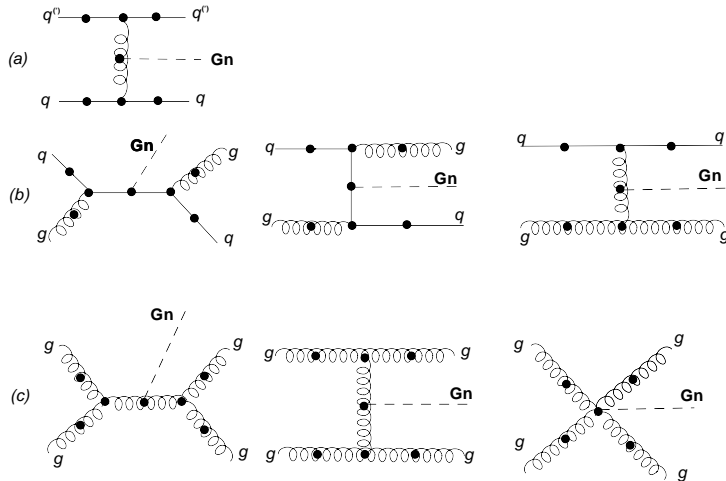


Figure 1: Representative Feynman diagrams for the subprocesses (a) $qq^{(l)} \rightarrow qq^{(l)}G_n$, (b) $qg \rightarrow qqG_n$, and (c) $gg \rightarrow ggG_n$ which contribute to the dijet plus graviton production process, $pp \rightarrow jjG_n + \text{anything}$. The gravitons are emitted from each of the solid points in the diagrams.

The signal and background are simulated at the parton level with full tree level matrix elements. The amplitudes are calculated by the helicity amplitude technique [11], and we have added all the relevant HELAS subroutines [12] for the massive graviton and its interactions based on the effective Lagrangian of Eq. (1.2). For the background, we used the codes based on Ref. [13] and checked by MadGraph/MadEvent [14]. For the signal, we have performed two independent calculations to check each other. Firstly, we wrote our simulation codes based on the ones generated for calculations of graviton radiation at linear colliders [15], which matches closely with similar other calculations [16]. Secondly, we have also implemented ADD spin-2 gravitons into MadGraph/MadEvent. We find agreement between the two independent calculations.

Additional checks were carried out for the Born level amplitude. The most useful check is provided by the Ward identities arising from general coordinate invariance, which constitutes an essential feature of any theory involving gravity. We can write the amplitude for the emission of any graviton in the form

$$A_n(k, p_i) = T^{\mu\nu}(k, p_i) \epsilon_{\mu\nu}^{(\vec{n})}(k), \quad (2.1)$$

where p_i are the momenta of the external SM particles, $\epsilon_{\mu\nu}^{(\vec{n})}(k)$ is the polarization tensor for the \vec{n} -th (massive) graviton mode with its momentum k . The tensor $T^{\mu\nu}(k, p_i)$ is the same for all the graviton modes, including the massless mode $\epsilon_{\mu\nu}^{(0)}(k)$, which is the graviton of the

four-dimensional Einstein gravity. This must now satisfy the Ward identities

$$k^\mu T_{\mu\nu}(k, p_i) = k^\nu T_{\mu\nu}(k, p_i) = 0, \quad (2.2)$$

where we note that

$$T^{\mu\nu}(k, p_i) = \sum_{j=1}^N T_j^{\mu\nu}(k, p_i) \quad (2.3)$$

with j indicating the j -th diagram, as above. The consistency check therefore requires a perfect cancellation between Feynman graphs, for each choice of μ or ν , which is highly sensitive to errors in signs and factors. Our numerical check in Ward identities confirms the cancellation up to the expected accuracy of our numerical programs.

Once dealing with this effective low-energy theory, one concern is its behavior above the ADD fundamental scale (M_s). One unitarity criterion which we have implemented is that the tower of gravitons being produced does not extend in mass beyond the ADD scale ($M_{G_n} < M_s$). Moreover, we will also present the results with a hard truncation scheme, by setting the cut $Q_{\text{truncation}} < M_s$, where the truncation parameter is set as the root of the partonic center-of-mass energy,

$$Q_{\text{truncation}} = \sqrt{\hat{s}}, \quad (2.4)$$

which is a quite conservative choice.

3. Results and Discussions

In the tree level numerical calculations, we identify massless partons with jets which must satisfy the angular cuts

$$\Delta R_{jj} = \sqrt{\Delta\eta^2 + \Delta\phi^2} > 0.7, \quad |\eta_j| < 4.5. \quad (3.1)$$

Here η is the pseudorapidity of the jets and ϕ is the azimuthal angle around the beam direction. Unless specified otherwise we further require

$$P_T^j > 6 \text{ GeV} \times \sqrt{P_T^{\text{miss}}/1 \text{ GeV}}, \quad (3.2)$$

$$P_T^{\text{miss}} > 1 \text{ TeV}. \quad (3.3)$$

We employ CTEQ6L1 parton distribution functions (PDF) [17] throughout, with the factorization scale chosen as $\mu_f = \min(P_T)$ of the jets which satisfy the above cuts. The QCD coupling is set to the geometric mean value, $\alpha_s = \sqrt{\alpha_s(P_T^{j1}) \alpha_s(P_T^{j2})}$. For the ADD parameter, we first focus on the $\delta = 4$ and $M_s = 5 \text{ TeV}$ case in Figs. 2-4, and then discuss the ADD scale sensitivity and present the differential distributions for $\delta = 3, 4, 5, 6$ cases, respectively. For $\delta > 6$ large extra dimensions, the total cross sections for real graviton production are smaller and not easy to detect at the LHC, thus we will not discuss them here.

Notice that throughout our calculations, we follow the notation of Ref. [3] which differs from the one in Ref. [4] mainly by a different factor in the relation between R and M_s in $(4+\delta)$ -dimensional space. Though this factor is crucial in comparing results and quantifying discovery potentials, one can simply convert results from one notation to the other by multiplying a δ -dependent factor.

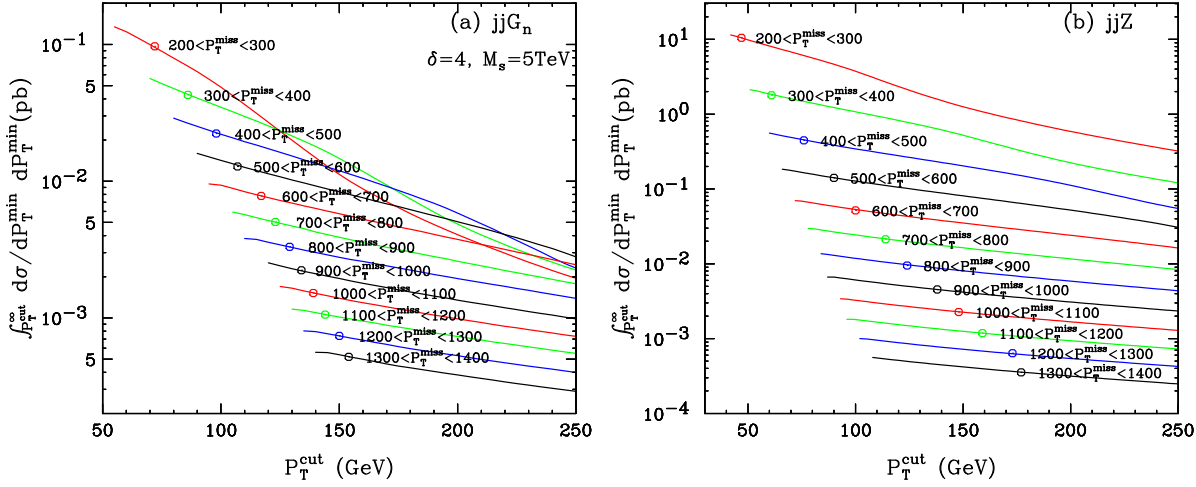


Figure 2: P_T^j cut dependence of the dijet cross sections for signal (a) and background (b) at the LHC in various missing transverse momentum bins when applying the cuts of Eq. (3.1). The open circles show the monojet cross section in the same missing P_T bin.

The P_T^j cut of Eq. (3.2) is chosen to insure perturbative ordering of the tree level cross sections throughout phase space, i.e. we want to keep the dijet cross sections below the corresponding 1-jet inclusive cross sections. In order to motivate our choice, we show, in Fig. 2, the P_T^j cut dependence of the total cross sections for the dijet plus missing P_T events at the LHC. Fig. 2(a) is for the signal process $pp \rightarrow jjG_n X$, and Fig. 2(b) is for the background process $pp \rightarrow jj(Z \rightarrow \nu\bar{\nu})X$. Each line shows the dijet cross section for the missing P_T in a 100 GeV bin between 200 GeV and 1400 GeV. The open circle along the lines shows the corresponding monojet cross section in the same missing P_T bin. In smaller P_T^{miss} bins, the jjG_n total cross sections drop faster, with increasing P_T^j cut, than the background ones, which is due to the soft and collinear Z boson emission along one of the QCD jet directions in the Zjj background.

The P_T^{min} values at open circle points in Figs. 2(a) and (b) tell the jet P_T threshold below which the dijet cross section is larger than the monojet cross section, and hence our perturbative results cannot be trusted. Below these threshold values one should expect multiple soft jet emission to appear. For a missing P_T of 1 TeV, for example, gluons with $P_T \lesssim 140$ GeV are in the soft range, and several such “soft” gluon jets are expected in a typical graviton or background

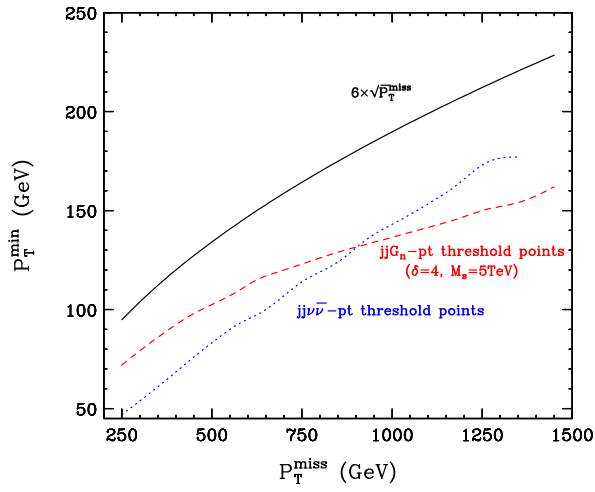


Figure 3: Missing transverse momentum dependence of the P_T^{cut} value of equal 2-jet and 1-jet cross sections. Our jet selection cut Eq. (3.2) is also presented.

event. Since these gluons are readily observable as distinct jets in the experiment, an actual monojet event with missing transverse momentum in the TeV range and no additional jets with $p_T \gtrsim 30$ GeV, is a very rare event.

To get results which are perturbatively reliable, we introduce the missing P_T dependent jet selection cut of Eq. (3.2) such that the dijet to monojet cross section ratio is always smaller than unity, while keeping as many dijet events as possible. We show in Fig. 3 our jet P_T cut of Eq. (3.2), together with the P_T threshold values for the signal (dashed red) and the background (dotted blue) above which the dijet cross section is smaller than the monojet one. We find from this figure that a larger fraction of graviton dijet events survives the cut for $P_T^{\text{miss}} \lesssim 900$ GeV, while $Z + \text{jet(s)}$ events obtain higher jet multiplicities at higher P_T^{miss} . This is partly because of the higher hard scattering scale of the graviton events at small P_T^{miss} , and partly because of the importance of collinear Z boson emission in high P_T^{miss} background events.

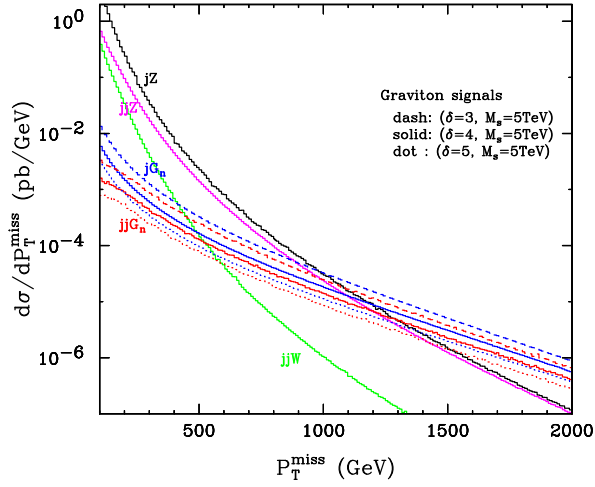


Figure 4: P_T^{miss} dependence of the total cross sections for the signal and background when applying the cuts of Eqs. (3.1), (3.2).

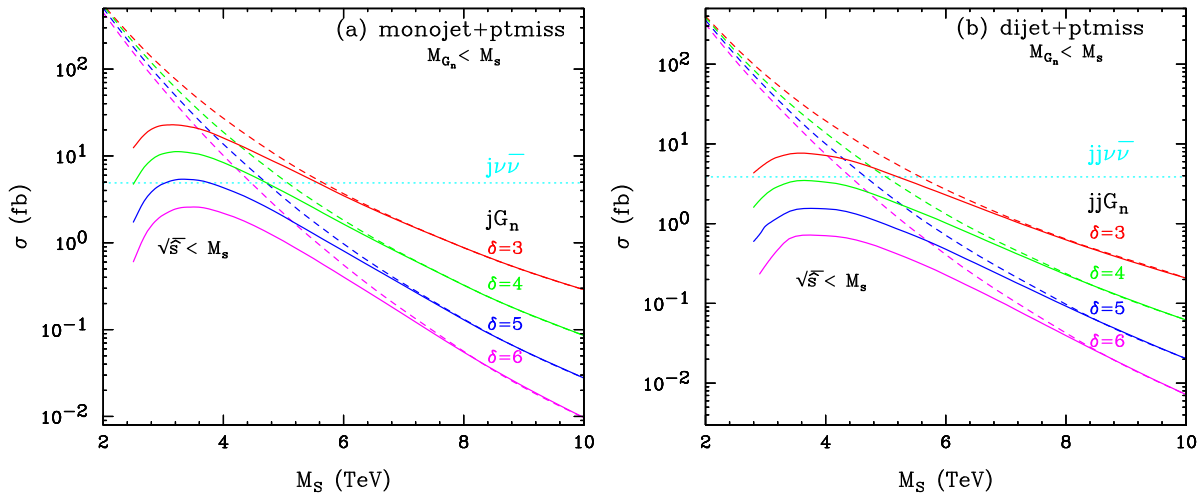


Figure 5: The dependence on ADD scale M_s of the total cross sections for jG_n (a) and jjG_n (b) productions at the LHC. The SM background results also have been plotted. The dashed lines are for $M_{G_n} < M_s$, while the solid lines are for $\sqrt{s} < M_s$. Event selection criteria chosen as in Eqs. (3.1) - (3.3).

In Fig. 4, we show the P_T^{miss} spectrum for both the 1-jet and 2-jets signal and background processes. One finds that the $P_T^{\text{miss}} > 1$ TeV requirement in Eq. (3.3) reduces the background

sufficiently. Also included is the contribution coming from the Wjj background which falls sharply for large P_T^{miss} and which yields an additional background contribution of 0.15 fb above $P_T^{\text{miss}} = 1$ TeV, i.e. it is negligible compared the the Zjj background. A further improvement of the signal to background ratio is possible by tightening the P_T^{miss} cut, but this will not be pursued in the following.

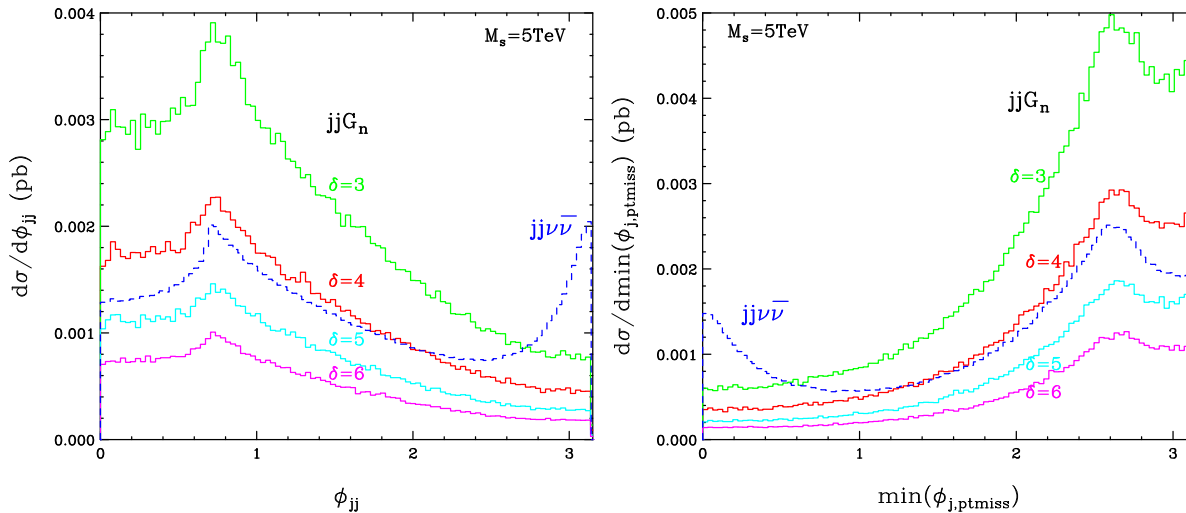


Figure 6: Distributions of the azimuthal angle separation between the two jets (left), and the minimal azimuthal angle separation between the two jets and missing transverse momentum (right), for background and graviton signal.

In Fig. 5, we present the ADD scale dependence of the total cross sections for jG_n and jjG_n production, for the $\delta = 3, 4, 5, 6$ cases. The SM $j\nu\bar{\nu}$ and $jj\nu\bar{\nu}$ background results are also plotted. Our results for jG_n production with the hard truncation scheme agree with the results in Ref. [3] within about 5 percent, which may be due to different PDF and scale choices. However, the results without truncation have larger differences especially at small M_s , because the unitarity criterion $M_{G_n} < M_s$ is used in our paper as mentioned above, while not in Ref. [3]. We have also performed the same sensitivity analysis as in Ref. [3], considering the integrated luminosity $\mathcal{L} = 100 \text{ fb}^{-1}$, where the systematic error in the background (assumed to be 10%) dominates over the statistical error. The sensitivity range is defined by

$$\sigma_{jjG_n}(\sigma_{jG_n}) > 5 \times 10\% \times \sigma_{\text{background}} = 1.93 \text{ (2.45) fb.} \quad (3.4)$$

The resulting max M_s sensitivity results are shown in table. I. The 2-jet sensitivity is only

δ	Max M_s sensitivity	Max M_s sensitivity
	$\mathcal{L} = 100 \text{ fb}^{-1}$	$\mathcal{L} = 100 \text{ fb}^{-1}$
	No truncation	Hard truncation
3	6.4 (6.6) TeV	6.3 (6.5) TeV
4	5.6 (5.7)	5.1 (5.5)
5	5.2 (5.3)	- (4.8)
6	4.9 (5.0)	- (3.6)

Table 1: Maximum ADD scale M_s sensitivity which can be reached by studying the 2-jet (1-jet) and missing transverse momentum signal at the LHC, with integrated luminosity $\mathcal{L} = 100 \text{ fb}^{-1}$, assuming the systematic error to be 10%.

slightly lower than for the 1-jet case. Moreover, the larger δ is, the sooner the non-perturbative region is reached, thus the larger is the difference between max M_s sensitivities in no truncation and hard truncation cases.

The most distinct difference between the signal and background in the dijet plus missing P_T events is found in azimuthal angle correlations between the 2 jets and the missing transverse momentum. The ϕ_{jj} and $\min(\phi_{j,P_T^{\text{miss}}})$ distributions with the cuts (3.1)-(3.3) are shown in Figs. 6, for $M_s = 5$ TeV and $\delta = 3, 4, 5, 6$, respectively. The Zjj background shows a clear enhancement for back to back jets, reflecting collinear Z emission along the direction of one of the jets. Due to the heavier masses of the typical graviton KK modes, such collinear “jet fragmentation” contributions are absent for the signal. This significant difference of the azimuthal angle distributions can provide a powerful tool to test for heavy graviton emission: the relative suppression of the jet fragmentation contribution in the data would be a direct sign for a very massive object as a source of the missing transverse momentum.

Finally, we would like to comment on the ratio of the 2-jet over the 1-jet rate. Since the typical graviton KK modes are much heavier than the Z boson, thus providing for a much harder event, one would expect naively that the ratio for the signal should always be larger than the one for the background. However, that is not the case as can be seen from the results in Fig. 4, especially at large P_T^{miss} . The reason can be traced back to final state parton emission, which is more prominent for the SM background. Based on this observation, we show, in Fig. 7, the 2-jet over 1-jet ratio for signal and background as a function of P_T^{miss} . The upper two curves are from the results in Fig. 4. For the lower two curves, we set additional cuts $|\Delta\eta_{jj}| > 2$ and $|\phi_{jj} - \pi| > 0.7$, in order to reduce final state parton emissions. One now finds a higher dijet fraction for the graviton events, largely from initial state radiation, reflecting the harder collision scale of the graviton emission events at all missing P_T .

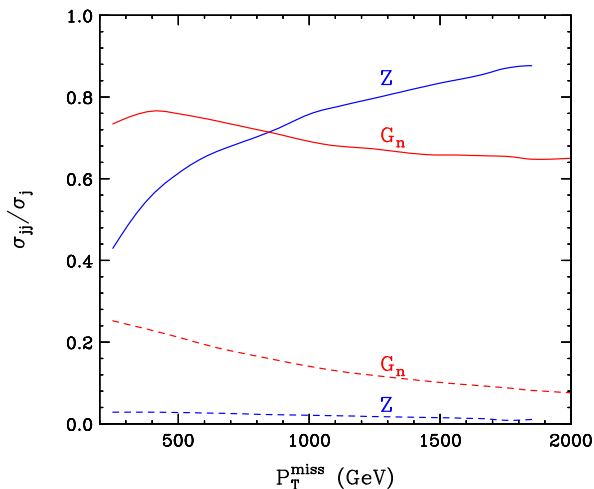


Figure 7: The 2-jet over 1-jet ratio for signal and background as a function of P_T^{miss} , with or without the cut $|\Delta\eta_{jj}| > 2$ and $|\phi_{jj} - \pi| > 0.7$. Additional cuts of Eqs. (3.1), (3.2) applied.

4. Summary

The production of stable Kaluza-Klein gravitons at the LHC can be observed when they are produced at large transverse momentum, giving rise to a large missing P_T signature. For P_T^{miss} of order 1 TeV or larger, the signature will rarely be a monojet signal, however, because multiple “soft” gluon emission will produce events with several jets balancing the transverse momentum of the graviton. We have calculated the order α_s^2 graviton plus dijet, jjG_n , cross section at the

LHC and find that it saturates the leading order monojet cross section for additional “soft” jet P_T in the 100 to 150 GeV range, thus establishing the typical scale for multiple jet emission.

The P_T^{miss} distribution of the jjG_n cross section is strongly influenced by the minimal jet p_T requirements imposed on the partons. We note that defining the dijet cross section with a typical constant jet P_T cut, independent of the hardness of the event, will invariably lead to the cross section not being trustworthy at sufficiently high P_T^{miss} , where saturation of the LO monojet cross section happens at higher jet P_T already. Not considering this effect, via a sliding jet P_T cut as in Eq. (3.2), may produce an unrealistically hard missing transverse momentum distribution, which can lead to an overestimate of the LHC sensitivity to graviton production.

In addition to the order α_s^2 process, jjG_n production via gluon exchange, we have also calculated the corresponding electroweak process $qq \rightarrow qqG_n$ via weak boson fusion. However, the cross section for the latter is always strongly suppressed. Even with typical weak boson fusion cuts we have been unable to find phase space regions where the electroweak process contributes to overall jjG_n production at more than the percent level, while also being visible above the SM background. We conclude that weak boson fusion is not a promising process for Kaluza-Klein graviton production at the LHC.

The multijet characteristics described above for the signal are also expected for the dominant SM background, Zjj production with subsequent decay of the Z boson to neutrino pairs. The multijet features are simply a reflection of the hardness of the event, as specified by the large missing transverse momentum. We have found one feature, however, which distinguishes signal and background processes. For missing P_T in the TeV range the Z mass becomes negligible and jet fragmentation into a collinear Z becomes an important part of the SM background. This contribution is most readily seen in the azimuthal angle correlations of the jets, with a sizable fraction of nearly back-to-back dijet events. The large average mass of the produced gravitons strongly suppresses such a contribution for the signal. The resulting distinctly different azimuthal angle distributions may be useful to verify that an observed excess of high P_T^{miss} events is indeed due to the production of an invisible very massive particle.

Acknowledgments

K. Hagiwara wishes to thank Michael Peskin for interesting discussions. P. Konar thanks Biswarup Mukhopadhyaya for his helpful suggestions. Q. Li and K. Mawatari would like to thank the KEK theory group for its warm hospitality. This work is supported in part by the Deutsche Forschungsgemeinschaft under SFB/TR-9 “Computergestützte Theoretische Teilchenphysik”, the core university program of JSPS, and the Grant-in-Aid for Scientific Research (No. 17540281) of MEXT, Japan and US Department of Energy under grant DE-FG02-97ER41029.

The Feynman diagrams in this paper were drawn using Jaxodraw [18].

References

- [1] N. Arkani-Hamed, S. Dimopoulos and G. Dvali, “The hierarchy problem and new dimensions at a millimeter,” *Phys. Lett. B* **429**, 263 (1998) [arXiv:hep-ph/9803315]; I. Antoniadis, N. Arkani-Hamed, S. Dimopoulos and G. Dvali, “New dimensions at a millimeter to a Fermi and superstrings at a TeV,” *Phys. Lett. B* **436**, 257 (1998) [arXiv:hep-ph/9804398]; N. Arkani-Hamed,

- S. Dimopoulos and G. Dvali, “Phenomenology, astrophysics and cosmology of theories with sub-millimeter dimensions and TeV scale quantum gravity,” *Phys. Rev. D* **59**, 086004 (1999) [arXiv:hep-ph/9807344].
- [2] E. G. Adelberger [EOT-WASH Group], “Sub-millimeter tests of the gravitational inverse square law,” [arXiv:hep-ex/0202008].
- [3] G. F. Giudice, R. Rattazzi and J. D. Wells, “Quantum gravity and extra dimensions at high-energy colliders,” *Nucl. Phys. B* **544**, 3 (1999) [arXiv:hep-ph/9811291].
- [4] T. Han, J. D. Lykken and R. J. Zhang, “On Kaluza-Klein states from large extra dimensions,” *Phys. Rev. D* **59**, 105006 (1999) [arXiv:hep-ph/9811350].
- [5] W. M. Yao *et al.* [Particle Data Group], “Review of particle physics,” *J. Phys. G* **33** (2006) 1.
- [6] LEP Exotica Working Group, LEP Exotica WG 2004-03.
- [7] A. Abulencia *et al.* [CDF Collaboration], “Search for large extra dimensions in the production of jets and missing transverse energy in p anti-p collisions at $s^{*(1/2)} = 1.96$ -TeV,” *Phys. Rev. Lett.* **97**, 171802 (2006) [arXiv:hep-ex/0605101].
- [8] L. Vacavant and I. Hinchliffe, “Signals Of Models With Large Extra Dimensions In Atlas,” *J. Phys. G* **27** (2001) 1839.
- [9] S. D. Ellis, R. Kleiss and W. J. Stirling, *Phys. Lett.* **154B**, 435 (1985); J. F. Gunion and Z. Kunszt, *Phys. Lett.* **161B**, 333 (1985); R. K. Ellis and R. J. Gonsalves, in *Proc. of the Workshop on super high energy physics*, Eugene, OR, 1985, ed. D. E. Soper, p. 287.
- [10] O. J. P. Eboli and D. Zeppenfeld, “Observing an invisible Higgs boson,” *Phys. Lett. B* **495**, 147 (2000) [arXiv:hep-ph/0009158].
- [11] K. Hagiwara and D. Zeppenfeld, “Helicity Amplitudes For Heavy Lepton Production In $E^+ E^-$ Annihilation,” *Nucl. Phys. B* **274**, 1 (1986); K. Hagiwara and D. Zeppenfeld, “Amplitudes for Multiparton Processes Involving a Current at $e^+ e^-$, $e^+ p$, and Hadron Colliders,” *Nucl. Phys. B* **313**, 560 (1989); T. Gleisberg, F. Krauss, K. T. Matchev, A. Schalicke, S. Schumann and G. Soff, “Helicity formalism for spin-2 particles,” *JHEP* **0309**, 001 (2003) [arXiv:hep-ph/0306182].
- [12] H. Murayama, I. Watanabe and K. Hagiwara, “HELAS: HELicity Amplitude Subroutines for Feynman diagram evaluations,” KEK-91-11, 1992.
- [13] V. D. Barger, T. Han, J. Ohnemus and D. Zeppenfeld, “Large $p(t)$ Weak Boson Production at the Tevatron,” *Phys. Rev. Lett.* **62**, 1971 (1989); V. D. Barger, T. Han, J. Ohnemus and D. Zeppenfeld, “Perturbative Qcd Calculations Of Weak Boson Production In Association With Jets At Hadron Colliders.” *Phys. Rev. D* **40**, 2888 (1989) [Erratum-ibid. *D* **41**, 1715 (1990)].
- [14] T. Stelzer and W. F. Long, “Automatic generation of tree level helicity amplitudes,” *Comput. Phys. Commun.* **81**, 357 (1994) [arXiv:hep-ph/9401258]; F. Maltoni and T. Stelzer, “MadEvent: Automatic event generation with MadGraph,” *JHEP* **0302**, 027 (2003) [arXiv:hep-ph/0208156]; J. Alwall *et al.*, “MadGraph/MadEvent v4: The New Web Generation,” *JHEP* **0709**, 028 (2007) [arXiv:0706.2334 [hep-ph]].
- [15] S. Dutta, P. Konar, B. Mukhopadhyaya and S. Raychaudhuri, “Bhabha scattering with radiated gravitons at linear colliders,” *Phys. Rev. D* **68**, 095005 (2003) [arXiv:hep-ph/0307117]; P. Konar and P. Roy, “Event shape discrimination of supersymmetry from large extra dimensions at a linear collider,” *Phys. Lett. B* **634**, 295 (2006) [arXiv:hep-ph/0509161].

- [16] T. Han, D. L. Rainwater and D. Zeppenfeld, “Drell-Yan plus missing energy as a signal for extra dimensions,” *Phys. Lett. B* **463**, 93 (1999) [arXiv:hep-ph/9905423]; O. J. P. Eboli, M. B. Magro, P. Mathews and P. G. Mercadante, “Direct signals for large extra dimensions in the production of fermion pairs at linear colliders,” *Phys. Rev. D* **64**, 035005 (2001) [arXiv:hep-ph/0103053].
- [17] J. Pumplin, D. R. Stump, J. Huston, H. L. Lai, P. Nadolsky and W. K. Tung, “New generation of parton distributions with uncertainties from global QCD analysis,” *JHEP* **0207**, 012 (2002) [arXiv:hep-ph/0201195].
- [18] D. Binosi and L. Theussl, “JaxoDraw: A graphical user interface for drawing Feynman diagrams,” *Comput. Phys. Commun.* **161**, 76 (2004) [arXiv:hep-ph/0309015].